Convex Optimization Techniques for Lunar Lander Trajectory Optimization

Christopher Davami*
Ethan Foss*
cdavami@ucsd.edu
erfoss@ucsd.edu
University of California, San Diego
San Diego, California, USA

KEYWORDS

Powered Decent Guidance, Moon Landing, Convex Optimization, Sequential Convex Programming, 6-DOF Guidance

ACM Reference Format:
Christopher Davami and Ethan Foss. 2024. Convex Optimization Techniques for Lunar Lander Trajectory Optimization. In *Proceedings of Convex Optimization (CSE 203B).* ACM, New York, NY, USA, 5 pages.

1 INTRODUCTION

1.1 Motivation

Lunar missions have received renewed interest in recent years, prompting the need for efficient algorithms that can compute fuel-optimal trajectories that guide spacecraft towards their mission objectives, specifically pinpoint landing. Convex optimization algorithms have become one of the most popular techniques for powered descent guidance for rocket landing, and we would like to demonstrate the viability of such techniques for a fuel-optimal lunar lander guidance.

1.2 Previous Works

In the context of celestial landing, real-time optimal powered descent is of interest. Solving the problem onboard quickly is necessary due to propellant restrictions and the nature of fuel-intensive retropropulsion systems, see Ref. [7]. This is a challenge when considering the nonlinear dynamics and nonconvex nature of the 6 degree-of-freedom (6-DOF) problem formulation, in which both the positional and rotational dynamics are considered. These challenges are only amplified when considering the deviations and corrections necessary for precision landing. The work on fuel-optimal powered descent guidance began during the Apollo program, see Refs[12, 17, 21, 22]. These approaches utilized optimal control theory, calculus of variations, or nonlinear programming [23, 24]. These methods proved too complicated and computers were numerically incapable for the time. The well-known Apollo Powered Descent Guidance (APDG) [16] was chosen for its simplicity, notably having a closed-form solution. While APDG was excellent for its time and has been flight proven on multiple missions [9, 14, 30], the guidance algorithm is not fuel-optimal. Traditional methods have been effective but may not exploit the full potential of modern optimization techniques. Considering the drastic increase of interest for Lunar missions, a fuel-optimal real-time guidance is desired to replace the 55-year old APDG.

Many works have taken different avenues to develop such a guidance algorithms. Upon the creation of interior point methods for numerical optimization, which guarantee convergence to a global optimum under the condition that the problem is convex, some took powered descent guidance methods in a new direction within direct methods, one towards convex optimization. Refs. [1–3, 6, 11, 15, 25, 31, 34] have all contributed to the convexification

Table 1: Tasks and Assigned Person(s)

Section	Task	Assignment
Introduction	Motivation	Ethan
Previous works	Lunar PDG background	Chris
	SCP background	Ethan
Contributions	Impacts of paper	Chris & Ethan
Organization	Editing & formatting	Chris & Ethan
Problem Statement	Primal formulation	Chris & Ethan
	Dual formulation	Chris & Ethan
	KKT conditions	Chris & Ethan
Approaches	SCP	Ethan
	Guidance & Simulation	Chris
Conclusions	Results	Chris & Ethan
	APDG vs SCP	Chris
	6-DOF Demo	Ethan
	Findings	Chris & Ethan
	Future work	Chris & Ethan
References		Chris & Ethan

*Both authors contributed equally to this research.

CSE 203B, March 21, 2024, University of California, San Diego

ACM ISBN 978-x-xxxx-xxxx-x/YY/MM…$15.00

of the 3-DOF powered descent problem, where only the positional dynamics of the lander are considered. The 6-DOF and mass varying 3-DOF problem formulations, however, do not have the same luxury of being represented as a convex problem due to the inclusion of nonconvex dynamics and constraints.

This is not the end of the story though, as convexification techniques have matured and successive convexification methods for iteratively solving nonconvex problems such as the 6-DOF powered descent problem have been developed. This is done by successively linearizing the dynamics and convexifying the constraints within a trust region. Many different methodologies for Successive Convex Programming exist, [19, 20, 27–29, 31, 32] but we will specifically employ the technique known as SCvx, which is outlined in detail in [20].

1.3 Intended Contributions

In this report, we have demonstrate a sequential convex programming algorithm for Apollo lunar descent guidance. The algorithm is formulated to be able to handle nonlinear dynamics and nonconvex constraints. We evaluate the performance of the algorithm for both 3-DOF guidance in a powered descent initialization scenario and 6-DOF guidance in a lunar surface landing point divert. In the 3-DOF scenario, we compare the performance of the SCP algorithm to the well established Apollo Powered Descent Guidance (APDG) algorithm and show that the SCP formulation is able to compute a trajectory that reduces the fuel consumption by 300 kg. For the 6-DOF guidance scenario, we develop a divert scenario in which the Apollo lunar lander must change landing location to the opposite side of a parabolic hill. Our results show that the SCP algorithm is an extremely promising candidate for future lunar landing missions.

Our unique contribution is the formulation of an SCP algorithm for the Apollo lunar lander and the comparison of this algorithm to other existing algorithms.

2 STATEMENT OF PROBLEM

The goal of an Apollo guidance scheme is to determine a trajectory, which is represented by a discrete sequence of states and inputs, that minimizes fuel expenditure. This trajectory must be dynamically feasible, that is it must satisfy the equations of motion. Moreover, the inputs to the system, the reaction control system (RCS) and descent propulsion system (DPS) thrusters must satisfy some thrust limits. Such a problem exists in a class of nonlinear programs, and is therefore difficult to solve.

To solve the Apollo trajectory optimization problem under a convex optimization framework, we employ a method known as Sequential Convex Programming (SCP), which performs a discretization of the nonlinear dynamics about a reference solution and solves a cone program over several iterations.

At each sub-iteration of the sequential convex program, we seek to solve a convex optimization problem that minimizes some objective related to the final state value subject to constraints involving the linear dynamics, linearized non-convex constraints, convex constraints, and boundary conditions. Since the dynamic linearization is performed about a possibly infeasible reference trajectory, virtual control is added to the dynamics to make the subproblem always feasible. Virtual terms are also added to the boundary conditions of the problem. Lastly, a trust region on the trajectory is enforced so that the trajectory cannot stray too far from its reference, meaning that the optimal solution is always bounded. With these relaxations, the convex subproblem is a second-order cone program that is always feasible and always bounded.

2.1 Primal Formulation

The optimization problem in 1 is a basic primal formulation of a sub-iteration of the SCP scheme. The parameters A_k, B_k, C_k, r_k are constant matrices that represent the linearized dynamics of the problem. Moreover, H_0, I_0, J_0, H_f, I_f, and J_f represent the boundary conditions of the problem. The solution variables are $\boldsymbol{x}_k$, the state of Apollo at each node point (i.e. the position, velocity and possibly quaternions and rotational rates), $\boldsymbol{u}_k$, the input of Apollo at each node point (i.e. the thruster values), p, a time scaling parameter, $\boldsymbol{\nu}_k$, the virtual control input at each node point, $\boldsymbol{\nu}_{ic}$, the initial condition relaxation parameter, and $\boldsymbol{\nu}_{tc}$ the final condition relaxation parameter. Other constant user-specified parameters include λ, the virtual control penalty, λ_{ic}, the initial condition slack penalty, λ_{tc}, the final condition slack penalty, and η, the trust region size. $\bar{\boldsymbol{x}}_k$, $\bar{\boldsymbol{u}}_k$, p, are constant parameters representing the reference trajectory at each node. The feasible input set can vary depending on the Apollo problem. For example, in the three degree-of-freedom formulation the input set a 2-norm constraints, whereas in the six degree-of-freedom formulation the input set is a linear inequality constraint. For the primal problem below we will consider the former.

$$
\begin{aligned}
\min_{\boldsymbol{x},\, \boldsymbol{u},\, p,\, \boldsymbol{\nu},\, \boldsymbol{\nu}_{ic},\, \boldsymbol{\nu}_{tc}} \quad & l^T \boldsymbol{x}_N + \lambda_{ic}\|\boldsymbol{\nu}_{ic}\|_2 + \lambda_{tc}\|\boldsymbol{\nu}_{tc}\|_2 + \lambda \sum_{k=1}^{N} \|\boldsymbol{\nu}_k\|_2 \\
\text{subject to} \quad & H_0 \boldsymbol{x}_1 + I_0 \boldsymbol{u}_1 + J_0 p + l_0 = \boldsymbol{\nu}_{ic} \\
& H_f \boldsymbol{x}_N + I_f \boldsymbol{u}_N + J_f p + l_f = \boldsymbol{\nu}_{tc} \\
& \boldsymbol{x}_{k+1} = A_k \boldsymbol{x}_k + B_k \boldsymbol{u}_k + C_k p + r_k + \boldsymbol{\nu}_k, \quad k = 1, 2, ..., N-1 \\
& \|\boldsymbol{u}_k\|_2 \le 1 \quad k = 1, 2, ..., N \\
& \|\boldsymbol{x}_k - \bar{\boldsymbol{x}}_k\|_2 + \|\boldsymbol{u}_k - \bar{\boldsymbol{u}}_k\|_2 + \|p - \bar{p}\|_2 \le \eta, \quad k = 1, 2, ..., N
\end{aligned} \tag{1}
$$

It is shown in the appendix that this primal formulation can be equivalently represented in the SOCP standard form using the overloaded notation for x

$$
\begin{aligned}
\min_{\boldsymbol{x}}, \quad & \boldsymbol{c}^T \boldsymbol{x} \\
\text{subject to} \quad & A\boldsymbol{x} = \boldsymbol{b} \\
& \|F_i \boldsymbol{x} + \boldsymbol{g}_i\|_2 \le \boldsymbol{h}_i^T \boldsymbol{x} + \boldsymbol{q}_i, \quad i = 1, 2, ..., M
\end{aligned} \tag{2}
$$

2.2 Dual Formulation

The Lagrangian of the SOCP with equality constraints from Eq. 2 is

$$
\begin{aligned}
L(\boldsymbol{x}, \boldsymbol{\lambda}, z, \boldsymbol{\omega}) = \boldsymbol{c}^T \boldsymbol{x} + \boldsymbol{\lambda}^T (A\boldsymbol{x} - \boldsymbol{b}) \\
- \sum z_i^T (F_i \boldsymbol{x} + \boldsymbol{g}_i) - \omega_i (\boldsymbol{h}_i^T \boldsymbol{x} - \boldsymbol{q}_i) \\
(\boldsymbol{z}_i, \boldsymbol{\omega}_i) \in K_i^*, i = 1, 2, ..., M
\end{aligned} \tag{3}
$$

The dual formulation is then determined by the infimum of the Lagrangian which gives the following dual problem

$$\begin{aligned} \max_{\boldsymbol{\lambda},\boldsymbol{z},\boldsymbol{\omega}} \quad & \boldsymbol{b}^T\boldsymbol{\lambda} - \sum_i \boldsymbol{g}_i^T \boldsymbol{z}_i + \boldsymbol{\omega}_i \boldsymbol{q}_i \\ \text{subject to} \quad & A^T\,\boldsymbol{\lambda} - \sum_i F_i^T \boldsymbol{z}_i - \boldsymbol{h}_i\boldsymbol{\omega}_i = \boldsymbol{c} \\ & \|\boldsymbol{z}_i\|_2 \le \boldsymbol{\omega}_i, \quad i = 1,2,\ldots,M \end{aligned} \tag{4}$$

2.3 KKT Conditions

Using the SOCP formulation, the KKT conditions are as follows

(1) Primal Feasibility:

$$\begin{aligned} & A\boldsymbol{x} = \boldsymbol{b} \\ & \|F_i\boldsymbol{x}_i + \boldsymbol{g}_i\|_2 \le \boldsymbol{h}_i^T\boldsymbol{x}_i + \boldsymbol{q}_i, \quad i = 1,2,\ldots,M \end{aligned} \tag{5}$$

(2) Dual Feasibility:

$$\begin{aligned} & A^T\,\boldsymbol{\lambda} - \sum_i F_i^T \boldsymbol{z}_i - \boldsymbol{h}_i\boldsymbol{\omega}_i = \boldsymbol{c} \\ & \|\boldsymbol{z}_i\|_2 \le \boldsymbol{\omega}_i, \quad i = 1,2,\ldots,M \end{aligned} \tag{6}$$

(3) Complimentary Condition:

$$\sum_i \boldsymbol{z}_i^T (F_i\boldsymbol{x} + \boldsymbol{g}) - \boldsymbol{\omega}_i(\boldsymbol{h}_i^T\boldsymbol{x} - \boldsymbol{q}_i) = 0, \quad i = 1,2,\ldots,M \tag{7}$$

(4) Stationary Condition:

$$\begin{aligned} \nabla_x L(\boldsymbol{x},\boldsymbol{\lambda},\boldsymbol{z},\boldsymbol{\omega}) = \boldsymbol{c} + A^T\boldsymbol{\lambda} - \sum F_i^T \boldsymbol{z}_i - \boldsymbol{\omega}_i\boldsymbol{h}_i = 0 \\ (\boldsymbol{z}_i, \boldsymbol{\omega}_i) \in K_i^*, \quad i = 1,2,\ldots,M \end{aligned} \tag{8}$$

3 INTENDED APPROACHES

3.1 Sequential Convex Program

Each convexified iteration's primal problem is solved using MOSEK. This optimizer uses the homogeneous interior-point algorithm, which offers a distinctive advantage over the primal-dual algorithm by reliably detecting potential primal or dual infeasibility [4]. The SCP algorithm was programmed in MATLAB using Yalmip as the convex program parsing tool. The dynamics are discretized using a first-order hold, and non-convex constraints are convexified by linearizing about the reference solution to approximate each non-convex constraint as a halfspace.

3.2 Guidance Comparisons and 6-DOF Capability Demonstrations

In order to accurately demonstrate the efficacy of SCP for lunar trajectory generation, a Lunar landing simulation using the Apollo 11 Lunar Module vehicle [33] is made using the 3-DOF Apollo approach and the 3-DOF SCP approach. The trajectories will be analyzed and the propellant consumption of each trajectory will be compared. Perfect navigation (the onboard estimation of the vehicle state is assumed to be 100% accurate) is assumed for all simulations. For the Apollo guidance the trajectory will use a closed-loop integrated trajectory where the thrust commands will be fed-back to the integrator every iteration. For more information on APDG thrust command generation see Refs. [16, 18]. The dynamics are non-stiff and nonlinear therefore the selected integrator is a 4th-Order Runge-Kutta. The guidance cycle for the APDG is 2 HZ. The SCP will usu the converged output of the guidance solution.

For the 6-DOF obstacle avoidance demo, we consider a hazard avoidance scenario upon touchdown. The safety system deems the present location unsafe and it must fly to a new location. Due to the presence of craters and mountains on the moon, it is necessary to avoid such obstacles. We model a mountain using a concave parabola. Recall that the successive convexification does not rely on the constraints to be convex. The Apollo LM 11 vehicle model within the SCP algortihm now adds reaction thrusters according to vehicle data in [33] to be used for attitude control.

4 RESULTS

4.1 SCP vs APDG

The following results use the identical initial conditions, final conditions, and vehicle model. The initial condition for the lunar simulation in a Cartesian frame with x in north, y in the east and z in the up direction are shown below in Table 2. The terminal condition is pinpoint landing that is zero terminal position and velocity.

Table 2: Simulation Initial Condition

x (m)	y (m)	z (m)	V_x (m/s)	V_y (m/s)	V_z (m/s)	m (kg)
-10,011	1,000	8,271	80	-20	-90	15,534

The APDG trajectory (shown in blue in Fig. 2) accurately achieves a pinpoint landing with a zero terminal velocity. The APDG uses around 1,949kg. The SCP (shown in orange in Fig. 2) also achieves the pinpoint landing with zero terminal velocity. However, the optimized solution only uses 319 kg less of propellant. It is important to note that this propellant savings is impactful not because the fuel is expensive but because of the valuable payload resources that this mass savings allows. The extra 319 kg of payload can be used for scientific tools, life-support systems for human missions, and extra safety measures thus improving the chances of lunar mission success. Though this added performance comes at the extra computational expense of carrying an optimization tool onboard, this trade-off is not of the same caliber as it was 55-years ago due to the numerical and computer hardware advances.

4.2 6-DOF Lunar Surface Divert

Lunar landing missions will inevitably encounter scenarios in which the landing site must be quickly changed due to obstacles that come in to view once the lander is close to the lunar surface. To demonstrate the ability of this algorithm to compute trajectories to avoid obstacles in a landing site divert scenario, we developed a 6-DOF divert in which a lunar lander has to move landing sites to the opposite side of a parabolic hill. In a short time frame divert, attitude dynamics are a necessary component of the trajectory optimization. This formulation creates additional nonconvexities due to the attitude dynamics and nonconvex input set which are handled by the SCP formulation by approximating each nonconvex constraint as a halfspace about the reference trajectory. The divert trajectory with the Apollo lunar lander plotted at each node point is shown in 3.

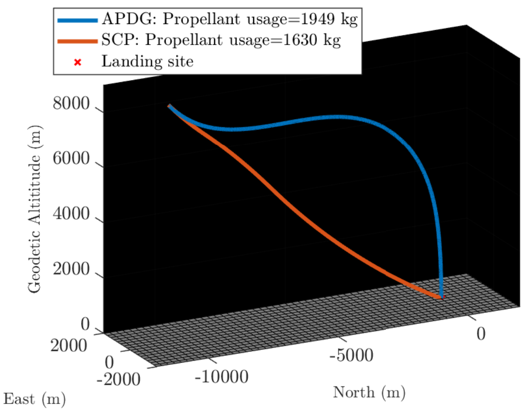

Figure 1: Lunar landing simulated trajectories for APDG and SCP algorithm.

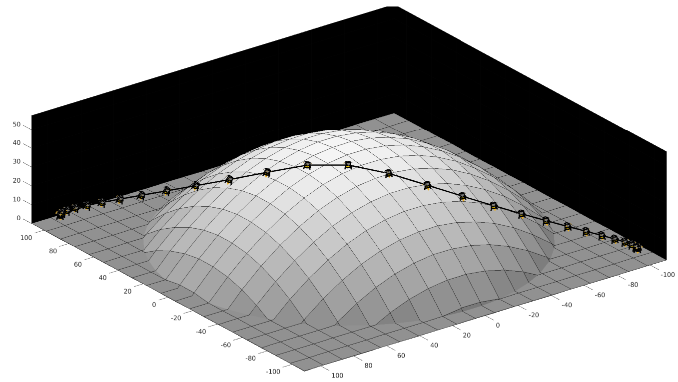

Figure 3: Fuel-Optimal 6-DOF Guidance of the Apollo Lunar Lander over a parabolic hill.

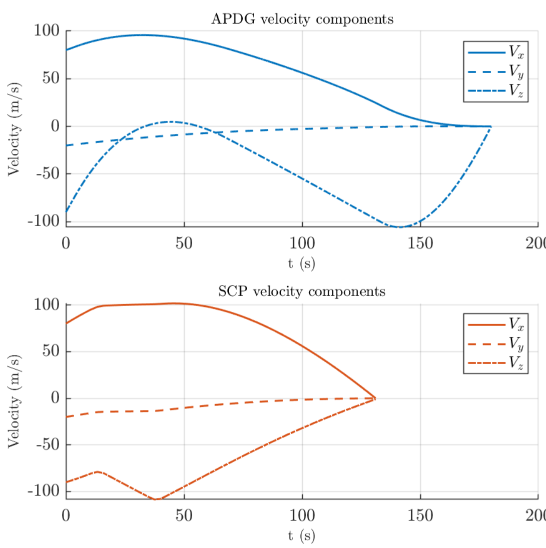

Figure 2: Lunar landing simulated velocity components for APDG and SCP algorithm.

5 CONCLUSION AND FUTURE WORK

In conclusion, this paper presents a novel approach to lunar lander descent guidance through the development and validation of a 6-DOF powered descent algorithm based on successive convex programming techniques. Our primary aim was to enable autonomous guidance of the lunar lander during descent while minimizing fuel usage and adhering to specified performance constraints. Through simulations and comparative analyses against the legacy Apollo Powered Descent Guidance system, we have demonstrated the efficacy of the SCP-based algorithm. Our results show significant fuel savings compared to the traditional APDG system, with the SCP algorithm achieving pinpoint landings with zero terminal velocity while using considerably less propellant. This reduction in propellant consumption not only enhances mission efficiency but also allows for increased payload capacity, thereby improving the feasibility and success rate of lunar missions. Furthermore, we showcased the capabilities of our algorithm in a 6-DOF obstacle avoidance scenario, highlighting its adaptability to complex lunar terrain and its potential to enhance mission safety. By successfully navigating around simulated obstacles, our algorithm showcases its versatility and effectiveness in real-world lunar landing scenarios.

Overall, the development and validation of the SCP-based descent guidance algorithm represent a significant advancement in lunar exploration technology. Convex optimization techniques and specifically successive convexification techniques have advanced the capabilities of Lunar landing guidance. We have demonstrated a viable upgrade to the existing APDG system, paving the way for more efficient and reliable lunar descent missions. Looking ahead, future research could focus on further refining the algorithm to handle even more complex terrain and environmental constraints. Additionally, integrating real-time adaptive control strategies such as Model Predictive Control (MPC) tracking (using a quadratic program) could further enhance the fidelity of the simulations and robustness of the descent guidance system against disturbances. With continued advancements in space exploration technology, the SCP-based descent guidance algorithm holds great promise for enabling safer, more efficient, and more ambitious lunar exploration missions in the years to come.

6 APPENDIX

6.1 Second Order Cone Program Reformulation

Here, we show that 1 can be reformulated as a second order cone program of the form 2. The solution variables are all vectorized into z with

$$z = [\boldsymbol{x}_1^T, \ldots \boldsymbol{x}_N^T, \boldsymbol{u}_1^T, \ldots \boldsymbol{u}_N^T, p, \boldsymbol{v}_1^T, \ldots \boldsymbol{v}_N^T, v_{ic}, v_{tc}, \boldsymbol{t}_x^T, \boldsymbol{t}_u^T, t_p, \boldsymbol{t}_k, t_{ic}, t_{tc}]^T \tag{9}$$

where the t's represent extra variables for epigraphs. 1 can be equivalently written as

$$
\begin{aligned}
\min_{z} \quad & l^T \boldsymbol{x}_N + \lambda_{ic} t_{ic} + \lambda_{tc} t_{tc} + \lambda \sum_{k=1}^{N} t_k \\
\text{subject to} \quad & \begin{bmatrix} \mathcal{A} & \mathcal{B} & C & \mathcal{E} & \mathbf{0} & \mathbf{0} & \mathbf{0} \\ \mathcal{H}_0 & \mathcal{I}_0 & \mathcal{J}_0 & \mathbf{0} & -I & \mathbf{0} & \mathbf{0} \\ \mathcal{H}_f & \mathcal{I}_f & \mathcal{J}_f & \mathbf{0} & \mathbf{0} & -I & \mathbf{0} \end{bmatrix} \boldsymbol{z} = \begin{bmatrix} -\boldsymbol{r} \\ l_0 \\ l_f \end{bmatrix} \\
& \|\boldsymbol{u}_k\|_2 \leq 1 \quad k = 1, 2, \ldots, N \\
& \|\boldsymbol{v}_{ic}\|_2 \leq t_{ic} \\
& \|\boldsymbol{v}_{tc}\|_2 \leq t_{tc} \\
& \|\boldsymbol{v}_k\|_2 \leq t_k, \quad k = 1, 2, \ldots, N \\
& \|\boldsymbol{x}_k - \bar{\boldsymbol{x}}_k\|_2 \leq t_{x,k}, \quad k = 1, 2, \ldots, N \\
& \|\boldsymbol{u}_k - \bar{\boldsymbol{u}}_k\|_2 \leq t_{u,k}, \quad k = 1, 2, \ldots, N \\
& \|\boldsymbol{p}_k - \bar{\boldsymbol{p}}_k\|_2 \leq t_p, \quad k = 1, 2, \ldots, N \\
& t_{x,k} + t_{u,k} + t_p \leq \eta, \quad k = 1, 2, \ldots, N
\end{aligned} \tag{10}
$$

The cost is now linear with respect to the solution variables. The equality constraints can be clearly written in the form $Az = b$. Then, by simply constructing matrices to select the specific variables that are present in the 2-norm constraints, each 2-norm constraint can be rewritten in a second-order cone form. Therefore, the optimization problem 1 can be rewritten equivalently in the form of 2.

REFERENCES

[1] Behçet Açıkmeşe, John M Carson, and Lars Blackmore. 2013. Lossless convexification of nonconvex control bound and pointing constraints of the soft landing optimal control problem. *IEEE Transactions on Control Systems Technology* 21, 6 (2013), 2104–2113.

[2] B Acikmese, J Casoliva, JM Carson, and L Blackmore. 2012. G-fold: A real-time implementable fuel optimal large divert guidance algorithm for planetary pinpoint landing. *Concepts and Approaches for Mars Exploration* 1679 (2012), 4193.

[3] Behcet Acikmese and Scott R Ploen. 2007. Convex programming approach to powered descent guidance for mars landing. *Journal of Guidance, Control, and Dynamics* 30, 5 (2007), 1353–1366.

[4] Erling D Andersen and Knud D Andersen. 2000. The MOSEK interior point optimizer for linear programming: an implementation of the homogeneous algorithm. In *High performance optimization*. Springer, 197–232.

[5] John T. Betts. 1998. Survey of Numerical Methods for Trajectory Optimization. *Journal of Guidance Control and Dynamics* 21 (1998). https://doi.org/10.2514/2.4231

[6] Lars Blackmore, Behçet Açikmeşe, and Daniel P Scharf. 2010. Minimum-landing-error powered-descent guidance for Mars landing using convex optimization. *Journal of guidance, control, and dynamics* 33, 4 (2010), 1161–1171.

[7] Robert D Braun, Brandon Sforzo, and Charles Campbell. 2017. Advancing supersonic retropropulsion using mars-relevant flight data: An overview. In *AIAA SPACE and Astronautics Forum and Exposition*. 5292.

[8] Peter L. Brodkin. 2021. *An Investigation of Optimal Powered Descent*. Master's thesis. University of Washington.

[9] Gilbert L Carman, Dallas G Ives, and David K Geller. 1998. Apollo-derived Mars precision lander guidance. In *AIAA, Atmospheric Flight Mechanics Conference and Exhibit, Boston, MA*.

[10] Yushu Chen, Guangwen Yang, Lu Wang, Haipeng Chen, Qingzhong Gan, and Quanyong Xu. 2023. A Fast Algorithm for Onboard Atmospheric Powered Descent Guidance. *IEEE Trans. Aerospace Electron. Systems* (2023).

[11] Bai Chengchao, Guo Jifeng, and Zheng Hongxing. 2018. Minimum-Fuel Powered Descent Guidance for Mars Landing. In *2018 9th International Conference on Mechanical and Aerospace Engineering (ICMAE)*. IEEE, 376–383.

[12] G Cherry. 1964. A general, explicit, optimizing guidance law for rocket-propelled spaceflight. In *Astrodynamics Guidance and Control Conference*. 638.

[13] Daniel Dueri, Behçet Açıkmeşe, Daniel P Scharf, and Matthew W Harris. 2017. Customized real-time interior-point methods for onboard powered-descent guidance. *Journal of Guidance, Control, and Dynamics* 40, 2 (2017), 197–212.

[14] Ingo Gerth and Erwin Mooij. 2014. Guidance for autonomous precision landing on atmosphereless bodies. In *AIAA Guidance, navigation, and control conference*. 0088.

[15] Matthew W Harris and Behçet Açıkmeşe. 2014. Maximum divert for planetary landing using convex optimization. *Journal of Optimization Theory and Applications* 162 (2014), 975–995.

[16] Allan R Klumpp. 1974. Apollo lunar descent guidance. *Automatica* 10, 2 (1974), 133–146.

[17] Derek F Lawden. 1963. Optimal trajectories for space navigation. *(No Title)* (1963).

[18] Ping Lu. 2020. Theory of fractional-polynomial powered descent guidance. *Journal of Guidance, Control, and Dynamics* 43, 3 (2020), 398–409.

[19] Danylo Malyuta. 2019. Discretization Performance and Accuracy Analysis for the Powered Descent Guidance Problem. (2019). https://doi.org/10.2514/6.2019-0925

[20] Danylo Malyuta. 2021. Convex Optimization for Trajectory Generation. (2021). https://doi.org/10.48550/arXiv.2106.09125

[21] J-P Marec. 1979. Optimal space trajectories. *NASA STI/Recon Technical Report A* 80 (1979), 48848.

[22] J Meditch. 1964. On the problem of optimal thrust programming for a lunar soft landing. *IEEE Trans. Automat. Control* 9, 4 (1964), 477–484.

[23] LS Pontryagin. 2018. *Mathematical Theory of Optimal Processes*. Routledge.

[24] Anil V Rao. 2009. A survey of numerical methods for optimal control. *Advances in the astronautical Sciences* 135, 1 (2009), 497–528.

[25] Taylor Reynolds, Danylo Malyuta, Mehran Mesbahi, Behcet Acikmese, and John M Carson. 2020. A real-time algorithm for non-convex powered descent guidance. In *AIAA Scitech 2020 Forum*. 0844.

[26] Taylor P. Reynolds. 2020. A Real-Time Algorithm for Non-Convex Powered Descent Guidance. (2020). https://doi.org/10.2514/6.2020-0844

[27] Jack Ridderhof and Panagiotis Tsiotras. 2019. Minimum-fuel powered descent in the presence of random disturbances. In *AIAA SciTech 2019 forum*. 0646.

[28] Jack Ridderhof and Panagiotis Tsiotras. 2021. Minimum-fuel closed-loop powered descent guidance with stochastically derived throttle margins. *Journal of Guidance, Control, and Dynamics* 44, 3 (2021), 537–547.

[29] Marco Sagliano, David Seelbinder, Stephan Theil, and Ping Lu. 2024. Six-Degree-of-Freedom Rocket Landing Optimization via Augmented Convex–Concave Decomposition. *Journal of Guidance, Control, and Dynamics* 47, 1 (Jan. 2024), 20–35. https://doi.org/10.2514/1.g007570

[30] Ronald Sostaric and Jeremy Rea. 2005. Powered descent guidance methods for the moon and mars. In *AIAA guidance, navigation, and control conference and exhibit*. 6287.

[31] Michael Szmuk, Taylor Reynolds, Behcet Acikmese, Mehran Mesbahi, and John M Carson. 2019. Successive convexification for 6-dof powered descent guidance with compound state-triggered constraints. In *AIAA Scitech 2019 Forum*. 0926.

[32] Michael Szmuk, Taylor P Reynolds, and Behçet Açıkmeşe. 2020. Successive convexification for real-time six-degree-of-freedom powered descent guidance with state-triggered constraints. *Journal of Guidance, Control, and Dynamics* 43, 8 (2020), 1399–1413.

[33] EMU DATA Technical Booklet. 1969. CSM/LM SPACECRAFT OPERATIONS, Vol iii: Mass properties. (1969).

[34] Ufuk Topcu, Jordi Casoliva, and Kenneth D Mease. 2007. Minimum-fuel powered descent for mars pinpoint landing. *Journal of Spacecraft and Rockets* 44, 2 (2007), 324–331.

[35] Runqiu Yang and Xinfu Liu. 2020. Fuel-optimal powered descent guidance with free final-time and path constraints. *Acta Astronautica* 172 (2020), 70–81.

Received 21 March 2024; revised 21 March 2024